Regular Article

RED CELLS, IRON, AND ERYTHROPOIESIS

Cell rigidity and shape override CD47's "self"-signaling in phagocytosis by hyperactivating myosin-II

Nisha G. Sosale,[1] Tahereh Rouhiparkouhi,[2] Andrew M. Bradshaw,[1] Rumiana Dimova,[2] Reinhard Lipowsky,[2] and Dennis E. Discher[1]

[1]Molecular and Cell Biophysics Laboratory, University of Pennsylvania, Philadelphia, PA; and [2]Max Planck Institute of Colloids and Interfaces, Potsdam, Germany

Key Points

- Rigidity of an opsonized red cell that contacts a macrophage is found to hyperactivate myosin-II and thus overpowers CD47's self-signaling.
- Red cell shape modulates CD47's signaling of self and highlights biophysical contributions to phagocytosis.

A macrophage engulfs another cell or foreign particle in an adhesive process that often activates myosin-II, unless the macrophage also engages "marker of self" CD47 that inhibits myosin. For many cell types, adhesion-induced activation of myosin-II is maximized by adhesion to a rigid rather than a flexible substrate. Here we demonstrate that rigidity of a phagocytosed cell also hyperactivates myosin-II, which locally overwhelms self-signaling at a phagocytic synapse. Cell stiffness is one among many factors including shape that changes in erythropoiesis, in senescence and in diseases ranging from inherited anemias and malaria to cancer. Controlled stiffening of normal human red blood cells (RBCs) in different shapes does not compromise CD47's interaction with the macrophage self-recognition receptor signal regulatory protein alpha (SIRPA). Uptake of antibody-opsonized RBCs is always fastest with rigid RBC discocytes, which also show that maximal active myosin-II at the synapse can dominate self-signaling by CD47. Rigid but rounded RBC stomatocytes signal self better than rigid RBC discocytes, highlighting the effects of shape on CD47 inhibition. Physical properties of phagocytic targets thus regulate self signaling, as is relevant to erythropoiesis, to clearance of rigid RBCs after blood storage, clearance of rigid pathological cells such as thalassemic or sickle cells, and even to interactions of soft/stiff cancer cells with macrophages. (*Blood*. 2015;125(3):542-552)

Introduction

Factors that promote the cytoskeleton-intensive process of phagocytosis (Figure 1A, left) are opposed by several inhibitory factors[1] that ultimately dictate whether a macrophage engulfs a target cell or particle. Immunoglobulin G (IgG) bound to a target engages the Fcγ receptor on a macrophage, for example, and this stimulates the assembly of numerous phagocytic synapse proteins,[2-4] including nonmuscle myosin-II motors that help drive uptake.[5-7] If CD47 is displayed in parallel on a target, it binds the macrophage's inhibitory receptor signal regulatory protein alpha (SIRPA),[8] which activates the immunomodulatory phosphatase Src homology region 2 domain-containing phosphatase-1 (SHP-1),[9] which regulates multiple proteins,[10] including suppression of nonmuscle myosin-IIA.[11] Inhibition of actomyosin contractility at the phagocytic synapse[7,12] could explain various observations that "marker of self" CD47 partially blocks phagocytosis of mouse red blood cells (RBCs),[13] as well as normal white blood cells,[14,15] stem cells,[16] and cancer cells.[16,17] Macrophage uptake of opsonized RBCs is also reported to contribute to clearance of RBCs in senescence[18-23] and in various diseases, including sickle cell anemia and thalassemia.[24,25] Such diseased cells and other conditions, including aging of cells, are the cause of many differences from normal that include increased cell rigidity,[26-28] increased IgG opsonization, increased phagocytosis, and in vivo processes consistent with increased clearance (supplemental Table 1, available on the *Blood* Web site). Remarkably, RBCs generated in culture from stem cells are phagocytosed independent of CD47 but in inverse proportion to elongation by shear,[29] and a ~50-fold increase in erythrocyte deformability during erythropoiesis had long been hypothesized to determine release of RBCs from marrow[30] where interactions with marrow macrophages occur in a niche known as the erythroblastic island.[31] Cell stiffness also changes in cancers and chemotherapy,[32-34] which could be important to broad anticancer efforts aiming to exploit CD47-SIRPA interactions.[12,17] Particle studies indeed show that stiff gel particles are engulfed in greater numbers than soft particles,[35] but relevance to cells with or without "self" is untested. Normal human RBCs are controllably stiffened here to assess phagocytosis of rigid self-cells under conditions that aim to preserve the interfacial biochemistry (Figure 1A, right).

As RBCs senesce, aldehydes are produced, which greatly accelerates RBC clearance from the circulation, but aldehyde levels are also higher in some diseased cells.[36,37] Aldehydes react primarily with amines in Lys residues, which only occur in CD47 distal to its binding site with SIRPA (Protein Data Bank ID code 2JJS). However, aldehydes can sometimes react with Arg,[38] which CD47 has in its binding site (Arg103), so that marker of self interactions might be inhibited by reaction with age-generated aldehydes. Aldehyde-mediated

Submitted June 27, 2014; accepted November 10, 2014. Prepublished online as *Blood* First Edition paper, November 19, 2014; DOI 10.1182/blood-2014-06-585299.

The online version of this article contains a data supplement.

The publication costs of this article were defrayed in part by page charge payment. Therefore, and solely to indicate this fact, this article is hereby marked "advertisement" in accordance with 18 USC section 1734.

cross-linking of various RBC membrane proteins certainly stiffens cells.[36] Rigid RBCs in healthy or disease states become stuck in narrow capillaries throughout the body,[39,40] especially splenic slits that impede rigid RBCs[41]; this could facilitate probing and clearance by splenic macrophages.[42] Synthetic polymer RBC mimics that lack any CD47 or other RBC proteins are also removed from circulating blood more rapidly when they are stiff compared with soft.[43]

Rigid cells that become physically lodged within blood vessels vs rigidity-enhanced phagocytosis have not been distinguished in past studies, and any role for CD47 in such processes is also unclear. The hypothesis examined here is that cell rigidity promotes phagocytic uptake by overwhelming CD47's signaling of self. Mechanistically, in the adhesion of most cell types to a planar substrate, a stiffer substrate generally activates myosin-II more so than a soft substrate; such activation drives polarization in hematopoietic stem cells,[44] cell spreading of macrophages[45] and neutrophils,[46] and actomyosin stress fiber assembly in various fibroblastic cell types.[47] However, whether rigidity-driven macrophage activation affects CD47 inhibition of phagocytosis has not been studied. Myosin-II is shown here to be hyperactivated by RBC rigidity and to oppose CD47's self-signaling, thereby increasing phagocytosis. The findings with cells of controlled rigidity and CD47 signaling are broadly relevant to erythropoiesis,[29] to accelerated senescence and clearance after blood storage,[48] to anemias that affect red cell shape and rigidity, to phagocytosis of cancer cells, and even to synthetic particles used in vivo.

Materials and methods

Reagents, cell lines, and standard methods are described in supplemental Methods. All blood was collected after informed consent with institutional review board approval at the University of Pennsylvania. This study was conducted in accordance with the Declaration of Helsinki.

Preparation of RBCs

Fresh RBCs were washed with phosphate-buffered saline (PBS), incubated with 0 to 50 mM glutaraldehyde (GA) for 1 minute at room temperature, and extensively washed. GA stomatocytes were first swollen with 200 mOsm PBS (30 minutes) and then treated with GA (50 mM, 200 mOsm, 1 minute, room temperature).

SIRPA binding assay

Soluble SIRPA-glutathione-*S*-transferase fusion (SIRPA-GST) was prepared and used as before with fluorescent anti-GST[47] or fluorescently labeled with AlexaFluor 546 maleimide (Life Technologies) (SIRPA-GST-Fluor). SIRPA-GST was incubated with RBCs for 30 minutes at room temperature. Cells were pelleted and resuspended in 5% fetal bovine serum/PBS, and intensity was measured by flow cytometry (Becton-Dickinson LSRII).

Phagocytosis assay by flow cytometry

For RBC opsonization, 10 μL packed RBCs were incubated with 0 to 10 μL opsonizing antibody (supplemental Table 2) and CD47 blocked with 0 to 270 nM anti-CD47 (B6H12). After shaking (Argos RotoFlex, 45 minutes, room temperature), RBCs were pelleted and labeled with PKH26 dye (room temperature, 30 minutes). THP-1–derived macrophages incubated with opsonized RBCs for standard phagocytosis assay[7] were isolated by washing cultures twice in PBS and 0.5 mL H_2O for RBC lysis (1 minute), followed by Trypsin incubation (5 minutes, 37°C) and quenching with RPMI. Macrophages were centrifuged (3000*g*, 5 minutes), resuspended with DNA labeling (10 minutes with Hoechst 33342), centrifuged again, and resuspended in 5% fetal bovine serum/PBS for flow cytometry analysis.

Results

Rigid human RBCs bind SIRPA but are rapidly engulfed

Normal human RBCs that are chemically modified with physiological concentrations of malonyldialdehyde[37] (MDA) or with GA display functional CD47 as demonstrated by binding soluble SIRPA-GST, as well as a function blocking anti-CD47 (Figure 1B; supplemental Figure 1). GA is just 2 carbons longer than MDA and is a common but hazardous disinfectant in the clinic.[49,50] Flow cytometry was used to measure binding and to also show that binding of soluble SIRPA-GST to RBCs could be inhibited by pretreatment of cells with the anti-CD47 (Figure 1B). Fluorescent SIRPA-GST (SIRPA-GST-Fluor) was used to image native and rigid RBCs (Figure 1C) and showed that SIRPA can still bind rigid RBCs, indicating that CD47 is likely folded correctly.

For rabbit RBC suspensions in fluid shear, the bulk deformability of cells decreases exponentially with aldehyde concentration[36] (supplemental Figure 2A). To assess cell-to-cell variability after GA treatment and on a scale similar to a phagocytic cup that forms in RBC engulfment, individual human RBCs (hRBCs) were aspirated here into micropipettes of slightly smaller diameter than the cells (Figure 1D). All native RBCs were rapidly aspirated and highly distorted, whereas GA RBCs always entered more slowly, deformed less, and, with extreme GA treatment, became stuck at the micropipette entrance (Figure 1D; supplemental Figure 2B). The exponential decrease in single cell deformability index with GA is consistent with past bulk results for aldehyde-treated RBCs in shear[36] (supplemental Figure 2A), and the reasonably small cell-to-cell variations indicate uniformity of the reaction. In addition, RBCs stored at room temperature for 1.5 days led to cell rigidification similar to a 17 mM GA treatment (Figure 1D, gray triangle). Such storage treatment is not as extreme as time-and-temperature treatments that are already known to drive rapid clearance by the spleen (ie, refrigerating at 4°C for >1 month or heating of RBCs to 50°C for 20 minutes[41]).

Fresh RBC discocytes normally possess a highly flexible membrane that extends easily under forces that even a few myosin motors might apply (~10 pN[27,51]). Time-lapse imaging of hRBCs opsonized with anti-human RBC antiserum during engulfment by human-derived THP-1 macrophages showed that CD47-blocked RBCs undergo classical phagocytosis, with uptake complete within 5 minutes after contact (Figure 2A). Erythrophagocytosis always begins with a macrophage pinching the RBC membrane into a semiconical synapse and causing the rest of the discocyte to become more spherical (Figure 2A-B; supplemental Figure 3A). Such pinching is also evident at the outset of phagocytosis of giant lipid vesicles that are subsequently ruptured (supplemental Figure 3B). With RBCs, macrophage pseudopods zipper along the membrane, constricting the erythrocytes in a manner expected to pressurize the hemoglobin-filled cytoplasm. Myosin-IIA contributes to cytoskeletal dynamics beneath the phagocytic cup,[6] and confocal imaging confirms that an engulfed RBC is quasi-spherical, with a diameter of ~6 μm, consistent with a sphere of conserved volume (supplemental Figure 3A, engulfed). When CD47 is not blocked (eg, native RBCs), such engulfment to spherical completion is infrequent (≤25%). More often, as CD47 signals self, macrophage-imposed deformations are larger and more sustained (Figure 2B). GA discocytes are not deformable and are rapidly engulfed (Figure 2C).

Regardless of self-signaling, extension of native RBCs that are being phagocytosed can provide estimates of forces that macrophages exert in engulfment (supplemental Figure 3C). Time-lapse

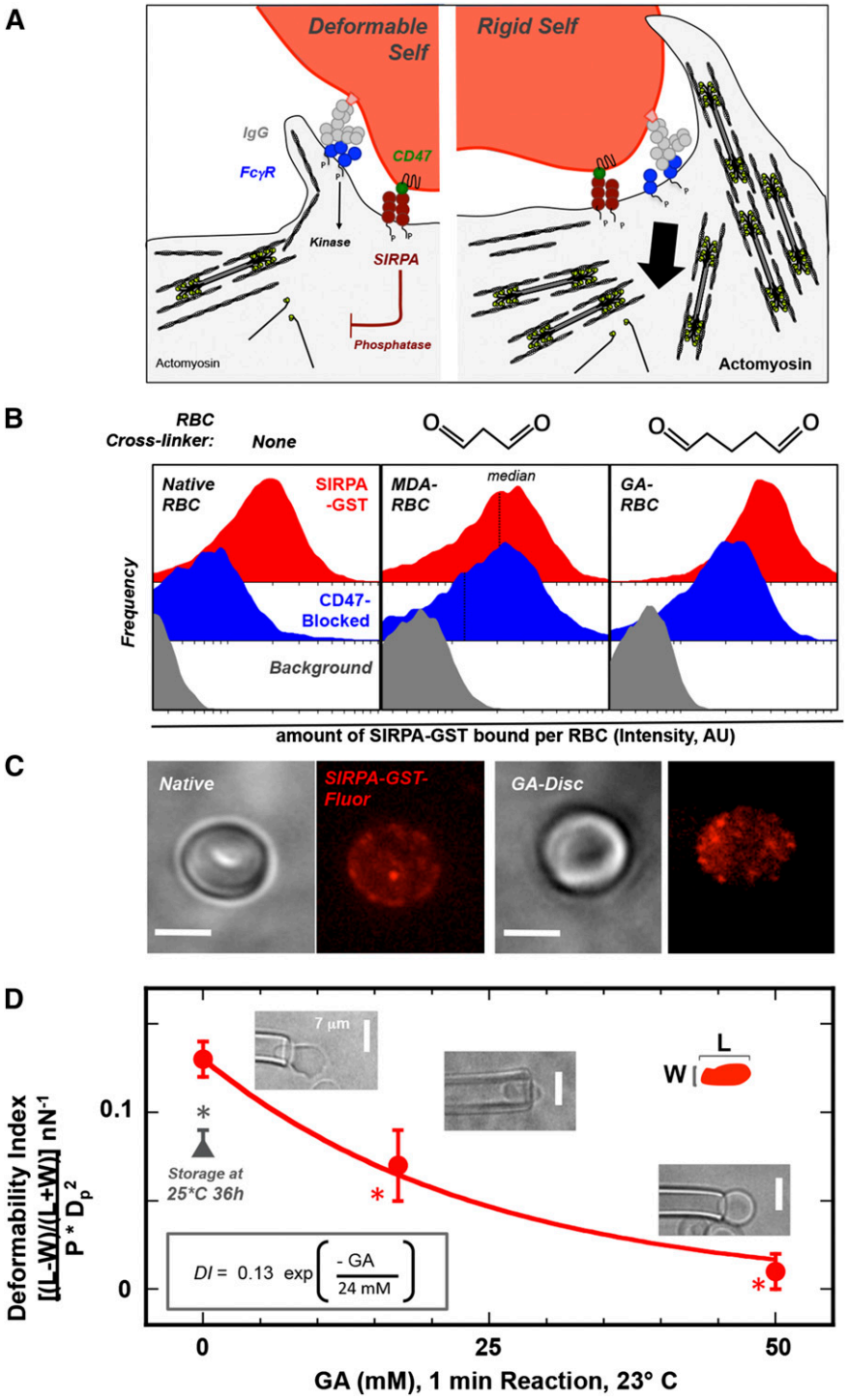

Figure 1. SIRPA binds CD47 on both rigid and native RBCs. (A) Downstream of FcγR binding of IgG, kinases phosphorylate multiple cytoskeletal proteins, including myosin-II, which drive assembly of the phagocytic cup and promote uptake. CD47-SIRPA signaling leads to activation of SHP-1 phosphatase that can deactivate myosin-II. Because substrate rigidity initiates assembly and polarization of myosin-II in many cell types, phagocytic target rigidity is expected to counterbalance CD47-mediated inhibition of the motor. Our working hypothesis is that with flexible self-cells (left), CD47 initiated inhibition can overcome myosin-II activation, whereas with rigid self-cells (right), the myosin-II driven cytoskeleton is not diminished by CD47-SIRPA self signals. (B) Flow cytometry histograms show SIRPA-GST binds to GA- and MDA-rigidified RBCs unless partially blocked by pretreating RBCs with anti-CD47. Cell aggregation by this antibody prevents a demonstration of complete inhibition. (C) SIRPA-GST-Fluor is covalently labeled with fluorophore and binds both native and aldehyde treated RBCs (scale bar, 5 μm). SIRPA-GST-Fluor was used to bind the MDA-RBCs in B, whereas anti-GST was used to detect binding on native and GA-RBCs. Supplemental Figure 1 further illustrates the saturable and specific binding, as well as CD47 blocking. (D) Aspiration of RBCs into micropipettes with diameters similar to phagocytic cups and in vivo capillaries shows GA treatment rigidifies cells, as does storage at ambient conditions. The maximal RBC length and width under aspiration were quantified by image analysis and normalized by pressure and pipette cross section (native, n = 9; 17 mM GA discocyte, n = 23; 50 mM GA discocyte, n = 2; error bar = standard deviation [SD]). *$P \leq .05$ compared with native; trend line $R^2 = 0.99$.

images were quantified most simply in terms of the RBC's projected length (L_p; Figure 2D, schematic, top left) along the phagocytosis axis and perpendicular to the synapse. L_p is initially ~8 μm, the diameter of an hRBC discocyte (Figure 2D). When CD47 is functionally signaling self, L_p increases up to ~12 μm, thus stretching the RBC by ~50%. Pseudopods extend from the macrophage but do not surround the RBC at the distal end; the RBC deformation process seems similar to that reported for macrophages pretreated with a myosin-light chain kinase inhibitor,[6] which will prove to be no coincidence. With GA-rigidified RBCs, the RBC is often flipped up and very rapidly engulfed, suggestive of rigidity-enhanced phagocytosis seen previously with polymer beads.[35] The GA RBCs contact the macrophage en face and seem to strongly adhere, but consistent with these GA discocytes being rigid, they do not become fully sphered in the phagosome as occurs with native RBCs (Figure 2C, inset fourth panel). GA discocytes are more often engulfed into spacious phagosomes with a ≤3-μm gap between discocyte and phagosome membranes (supplemental Figure 3D). The frequency of classical phagocytosis events, in which engulfment vectors inward and the RBC does not greatly stretch, is 100% for GA discocytes and 75% for CD47-blocked native RBCs vs ≤25% for native RBCs signaling self, with such frequency proportional to engulfment time (Figure 2E).

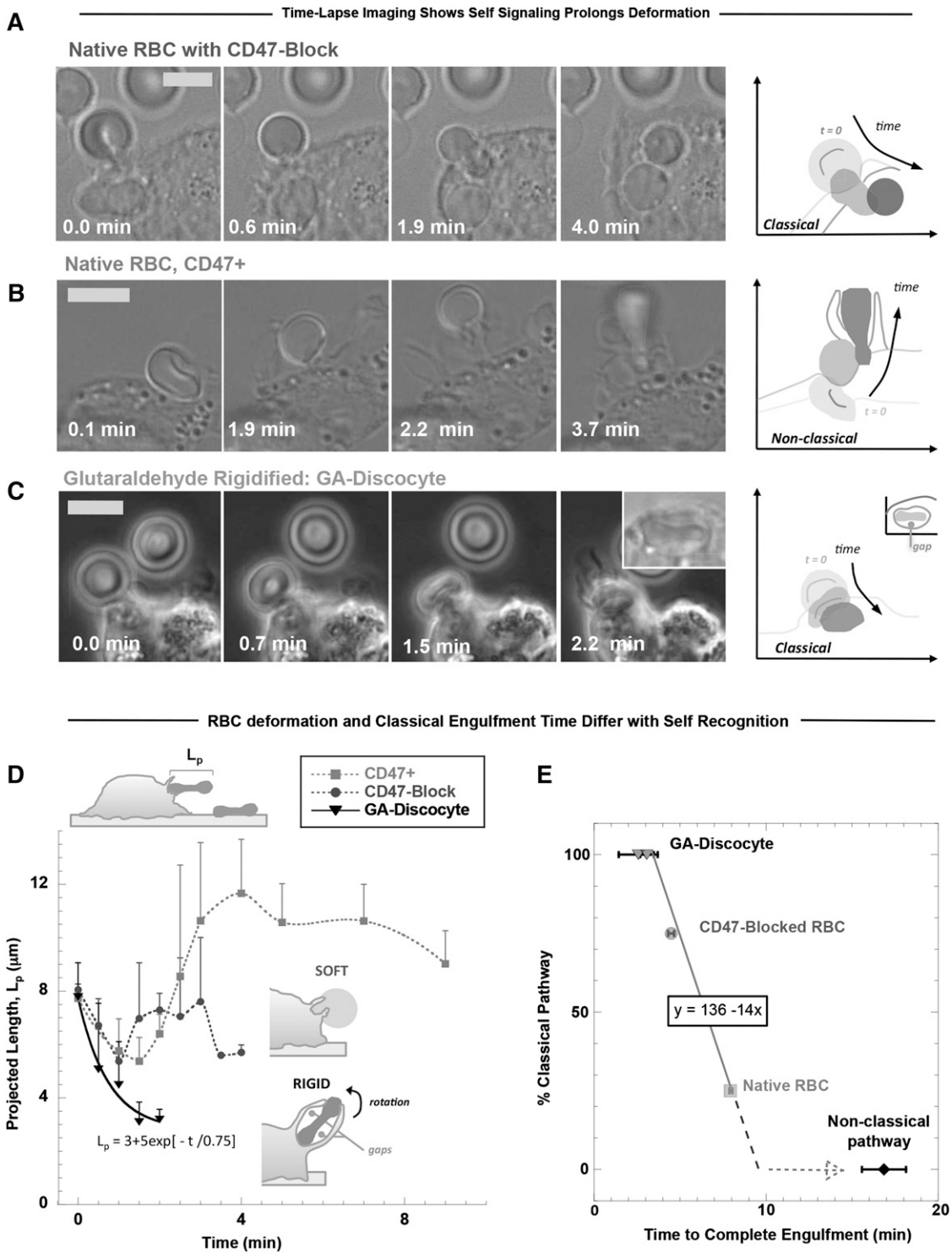

Figure 2. Phagocytic uptake of opsonized RBCs is faster with CD47 inhibition but fastest for rigid RBCs. Human-derived THP-1 macrophages were incubated with human RBCs that were opsonized with anti-hRBC antiserum and also (A) blocked with anti-CD47, (B) native RBCs with active CD47$^+$, or (C) rigidified as GA discocytes. Time-lapse imaging in DIC and phase contrast begins with initial adhesion between macrophage and RBC targets and ends on complete engulfment (scale bar, 8 μm). At the right of each time-lapse series, silhouettes of the target RBC clarify the changes in RBC morphology over the course of engulfment and RBC position relative to the macrophage boundaries, as indicated by the sketched lines (C, fourth panel, inset) GA discocytes are often enclosed in a spacious phagosome that shows gaps between the discocyte and phagosome membranes. (D) The projected length (L_p) of the engulfed RBC was quantified along the phagocytosis axis (schematic, top left) and shows that phagocytic deformation is fast and classically vectored inward for rigid RBCs and for CD47-blocked RBCs compared with native RBCs ($n \geq 3 \pm$ SD). When CD47 can signal self, phagocytosis is much slower, and L_p often increases (up to 1.5-fold L_{p0}). (E) The percentage of classical uptake events for each RBC treatment is plotted vs the time required to complete engulfment, with the frequency of classical uptake showing a negative linear correlation with engulfment time (line fit, $R^2 = 1.0$). Nonclassical uptake is most frequently observed with native RBCs that signal self and deviates from the classical trend by at least twofold.

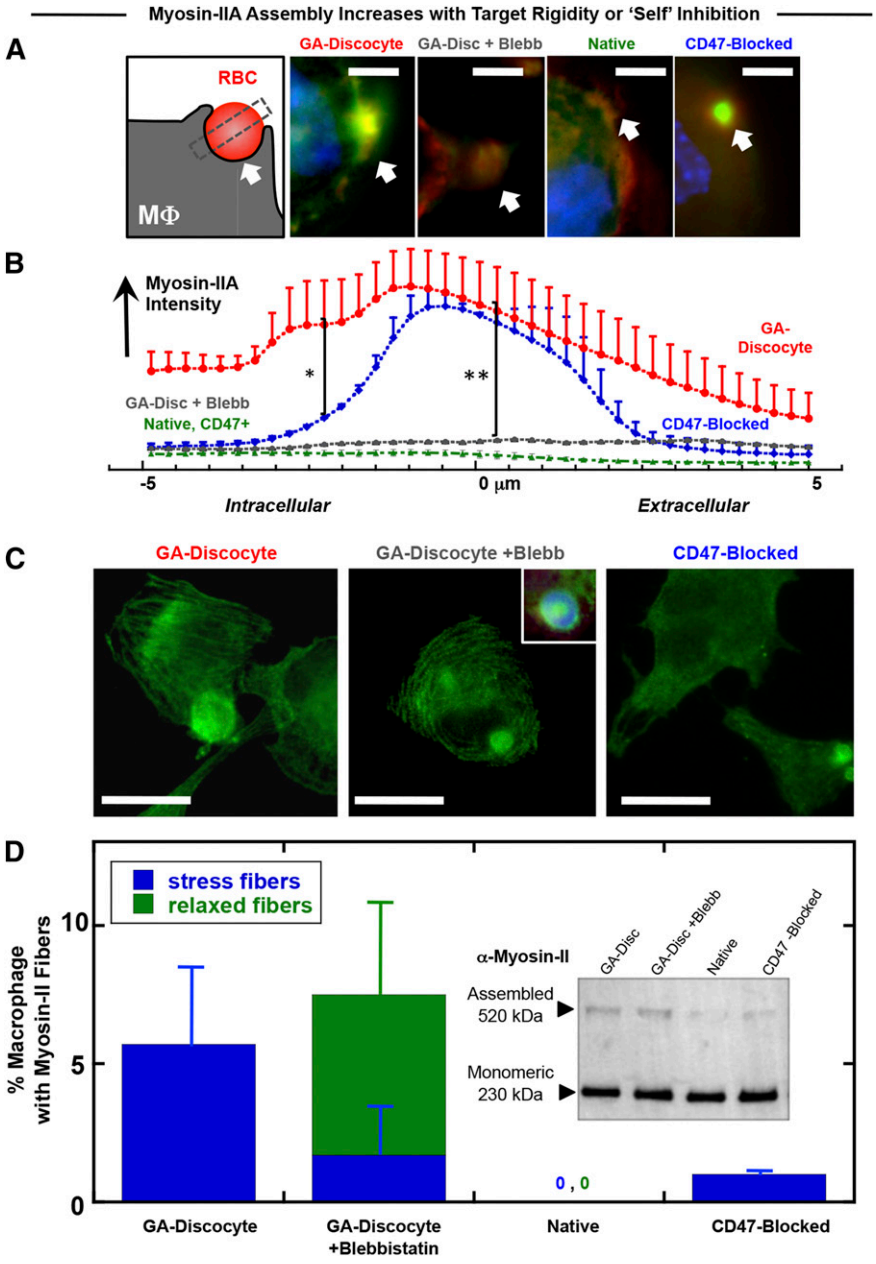

Figure 3. Myosin-II accumulation at the phagocytic synapse is strongly promoted by target rigidity and more weakly inhibited by CD47. (A) The phagocytic synapse schematic (left) illustrates the intensity analysis of immunofluorescence images. White arrow indicates alignment. THP-1 macrophages were either pretreated or not with myosin-II inhibitor blebbistatin (20 μM), followed by incubation with the various antiserum opsonized RBCs for 45 minutes at 37°C and then fixed and immunostained for myosin-IIA (green), F-actin (red), and DNA (blue) (scale bar, 10 μm). (B) Accumulation of myosin-II at the phagocytic synapse was quantified ($n \geq 3 \pm$ SD), proving highest for rigid GA discocytes and secondarily for CD47-blocked RBCs ($^*P < .05$). Blebbistatin suppresses myosin-IIA accumulation to levels similar to native RBCs, denoted $CD47^+$ ($^{**}P < .05$). (C) Fluorescence images of myosin-IIA localization in macrophage fed either GA discocytes with or without pretreatment with blebbistatin (20 μM), or CD47-blocked RBCs (scale bar, 30 μm). (D) Actomyosin fiber formation was quantified in macrophages, showing that addition of GA discocytes resulted in the highest frequency of macrophages with stress fibers. Blebbistatin pretreated macrophages showed curved and relaxed fibers, whereas macrophages cultured with native RBCs do not show fibers. (Inset) Immunoblot for nonmuscle myosin-IIA heavy chain, of macrophage lysates following phagocytosis, shows the presence of 230- and 520-kDa bands, with the high molecular weight band suggesting stable myosin assembly.

Importantly, with native RBCs, the process is most often nonclassical, with large distensions persisting approximately twofold longer than classical uptake and approximately fivefold longer than uptake of rigid RBCs.

Myosin-II localization to the phagocytic synapse is promoted by RBC rigidity

Adhesion to a rigid (not soft) substrate for many cell types drives cell spreading with assembly of stress fibers and polarization of nonmuscle myosin-II[44,46,52,53]; macrophages are certainly mechanosensitive in adhesion[45,54,55] and phagocytosis.[35] Target rigidity can therefore contribute to the generation of contractile forces during the phagocytosis of foreign cells. Accumulation of myosin-IIA at the phagocytic synapse between THP-1 macrophages and opsonized hRBCs is largely inhibited by CD47,[7] as reproduced in a comparison of CD47-blocked native hRBCs and native hRBCs (Figure 3A-B). Rigid GA discocytes, in comparison with native RBCs, show significantly greater accumulation of myosin-IIA within the macrophage distal to the human-human phagocytic synapse, and this apparent hyperactivation of contractility is completely inhibited by the myosin-II ATPase inhibitor blebbistatin (Figure 3A-B).

Actomyosin stress fibers are common with cells such as fibroblasts when adherent to rigid substrates, but stress fibers are found in only the occasional macrophage,[56] as is evident here in the rare THP-1 cell (supplemental Figure 4A-B). Surprisingly, addition of opsonized and rigid GA discocytes caused a larger fraction of cells to assemble stress fibers, unlike when native hRBCs were added in identical numbers (Figure 3C-D). Compared with native hRBCs that were CD47 blocked, rigid GA discocytes induced the formation of straight and tensed[57] stress fibers in fourfold more macrophages, whereas addition of blebbistatin produced relaxed arcs as seen in similarly treated myocytes.[58] Stress fibers were also induced in macrophages when CD47 was blocked (supplemental Figure 4A). Immunoblots

against the myosin-IIA heavy chain in whole cell lysates after phagocytosis indeed show a high-molecular-weight form of myosin-IIA (Figure 3D, inset) that suggests a greater assembly of myosin induced by rigid compared with native RBCs (supplemental Figure 4C). Rigidity of a phagocytic target thus tends to hyperactivate myosin-IIA in macrophages.

Rigid discocytes are phagocytosed in greater numbers than flexible discocytes

Although the studies above (Figures 1 to 3) all indicate engulfment processes depend functionally on RBC rigidity and CD47, complete engulfment is the definitive end stage and must be quantified. In addition, varying the level of opsonization is needed to demonstrate the net balance for and against phagocytic uptake. RBCs in dogs and humans are opsonized by autologous IgG[59] that increases up to sevenfold toward the end of the cell's life span in vivo,[19,60] and aged hRBCs lack other "eat me" signals, such as exposed phosphatidylserine.[61] Engulfment of native hRBCs by THP-1 macrophages is found to increase here with opsonization of the hRBCs by anti-hRBC antiserum, saturating at >10-fold higher levels than unopsonized hRBCs (Figure 4A). IgG concentration in serum is 100 μM, and the highest IgG concentration used here has been calculated to be 10 μM, with only a minor fraction of this expected to be specific for human RBCs (supplemental Table 2). Direct imaging of engulfed RBCs per macrophage at the end of the 45-minute in vitro assay was done by scoring ≥100 randomly chosen macrophages. For higher throughput, a flow cytometry assay was developed ("Materials and methods") and yielded the same relative phagocytic index as microscopy, with normalization to uptake of native RBCs. Blocking hCD47 nearly doubles the uptake of native cells that are highly opsonized, but blebbistatin inhibition of myosin-II always produces uptake levels statistically similar to native hRBCs (Figure 4B, left). Rigidified GA discocytes are engulfed at similar levels as CD47-blocked native RBCs (Figure 4B, right), whereas decreasing the GA treatment decreases phagocytosis (supplemental Figure 4D), similar to previously published results with MDA (supplemental Figure 4E), and follows an exponential trend consistent with the aldehyde dependence of rigidification (Figure 1D) and in vivo clearance (supplemental Figure 2A). Remarkably, blocking CD47 on the rigid GA discocytes consistently shows no effect on engulfment (Figure 4B, right; supplemental Figure 4F). In contrast, blebbistatin always inhibits uptake of GA discocytes (Figure 4B, far right), with phagocytosis reduced to levels similar to native RBCs that signal self. Increased uptake of GA discocytes and CD47-blocked RBCs thus depends largely on active myosin-II.

Varying the level of opsonization by antiserum helps reveal the mechanistic interplay of rigidity sensing and CD47 signaling (supplemental Figure 4G-H). At high antiserum opsonization (supplemental Table 2; Figure 4Ci), increasing amounts of anti-CD47 blocking promotes engulfment of native RBCs, saturating near the invariant level for GA discocytes. At low antiserum opsonization (Figure 4Cii), engulfment of native RBCs is minimal, with the same increases in anti-CD47 blocking, which indicates that the blocking antibody is not sufficiently abundant to contribute to opsonization. Conversely, the same low opsonization of GA discocytes increases engulfment with increasing anti-CD47 (Figure 4Cii, upper curve). Importantly, because the engulfment curves with anti-CD47 for native hRBCs with high antiserum (Figure 4Ci) and for rigid RBCs with low antiserum (Figure 4Cii) fit to the same saturable uptake curves, hCD47 appears equally functional on GA-treated cells. This conclusion from phagocytosis is consistent with binding to soluble SIRPA-GST (supplemental Figure 1A,C).

For zero antiserum (Figure 4Ciii), engulfment is always much lower, as expected. However, rigid GA discocytes are again engulfed more than native RBCs, and blocking with anti-CD47 decreases engulfment of rigid GA discocytes without affecting engulfment of native RBCs. The blocking results for rigid GA RBCs provides additional evidence that CD47 is functional, and because blocking impedes weakly adhesive interactions with macrophage SIRPA,[7] the result seems consistent with past reports of CD47 acting as an adhesive ligand for cell tethering and phagocytosis of apoptotic and/or damaged cells,[62] although any cell stiffness in the cited studies were not addressed.

GA discocytes with intermediate opsonization (supplemental Table 2) were used to clarify the mechanistic balance between pro- and antiphagocytic signals, starting with preincubation of macrophages with an anti-SIRPA antibody that blocks CD47-SIRPA interactions (Figure 4D). This leads to engulfment of rigid RBCs that is statistically the same as complete blocking with anti-hCD47. Because CD47 binding to SIRPA activates the phosphatase SHP-1, which we have shown[7] deactivates myosin-IIA at a phagocytic synapse with native RBCs, an inhibitor of SHP-1 (NSC8787712) was added and found to enhance uptake even more than the blocking antibodies (Figure 4D). This could reflect a basal level of SIRPA phosphorylation and signaling.[7]

We previously showed NOD/SCID/Il2rg$^{-/-}$ (NSG) mice recognize hCD47 as self, which is evident in slower splenic clearance when hCD47 is displayed.[12] Therefore, we injected stiff, highly opsonized hRBCs into NSG mice to examine splenic clearance. Blocking or not with anti-hCD47 had no effect on splenic macrophage uptake (Figure 4E; supplemental Figure 4I), which is consistent with our in vitro results (Figure 4C).

RBC shape also modulates engulfment

Changes in RBC shape during phagocytosis clearly decrease with RBC stiffness (Figure 2C), but whether the initial shape of the RBC influences engulfment and CD47 signaling is unclear and is certainly relevant to altered RBC shape in hereditary anemias (eg, hereditary spherocytosis and sickle cells[26]) and senescence.[22] Moreover, because rigid polystyrene spheres displaying CD47 can signal self and inhibit phagocytosis,[7,12] we generated and assayed more rounded and rigid RBCs. By treating RBCs with a mild hypotonic buffer prior to GA cross-linking, cells take on a morphology similar to that seen in hereditary stomatocytosis[24,63] (supplemental Figure 5A). In patients, stomatocyte-spleen interactions were abnormally high but also reduced by a drug that decreases production of tumor necrosis factor-α,[64] which is often associated with upregulation of adhesion molecules on vascular endothelium.[65]

In the absence of opsonization, the hypotonic pretreatment has no effect on the low basal level of phagocytosis of rigidified cells (Figure 5A). However, high antiserum increases phagocytosis in the order native < GA stomatocytes < GA discocytes (Figure 5A), even though opsonization is equal across the cells (supplemental Figure 5B). The hypotonic treatment is therefore indeed mild rather than damaging. Rigid GA stomatocytes bind soluble SIRPA-GST (supplemental Figure 5C) and signal self based on the observation that engulfment numbers increase with anti-CD47 blocking with opsonization by high antiserum (Figure 5B) and by purified anti-hRBC IgG (supplemental Figure 5D). As with native RBCs, immunoblocking of CD47 on GA stomatocytes also increases the rate of engulfment (supplemental Figure 5E). Nonetheless, inhibitory signaling

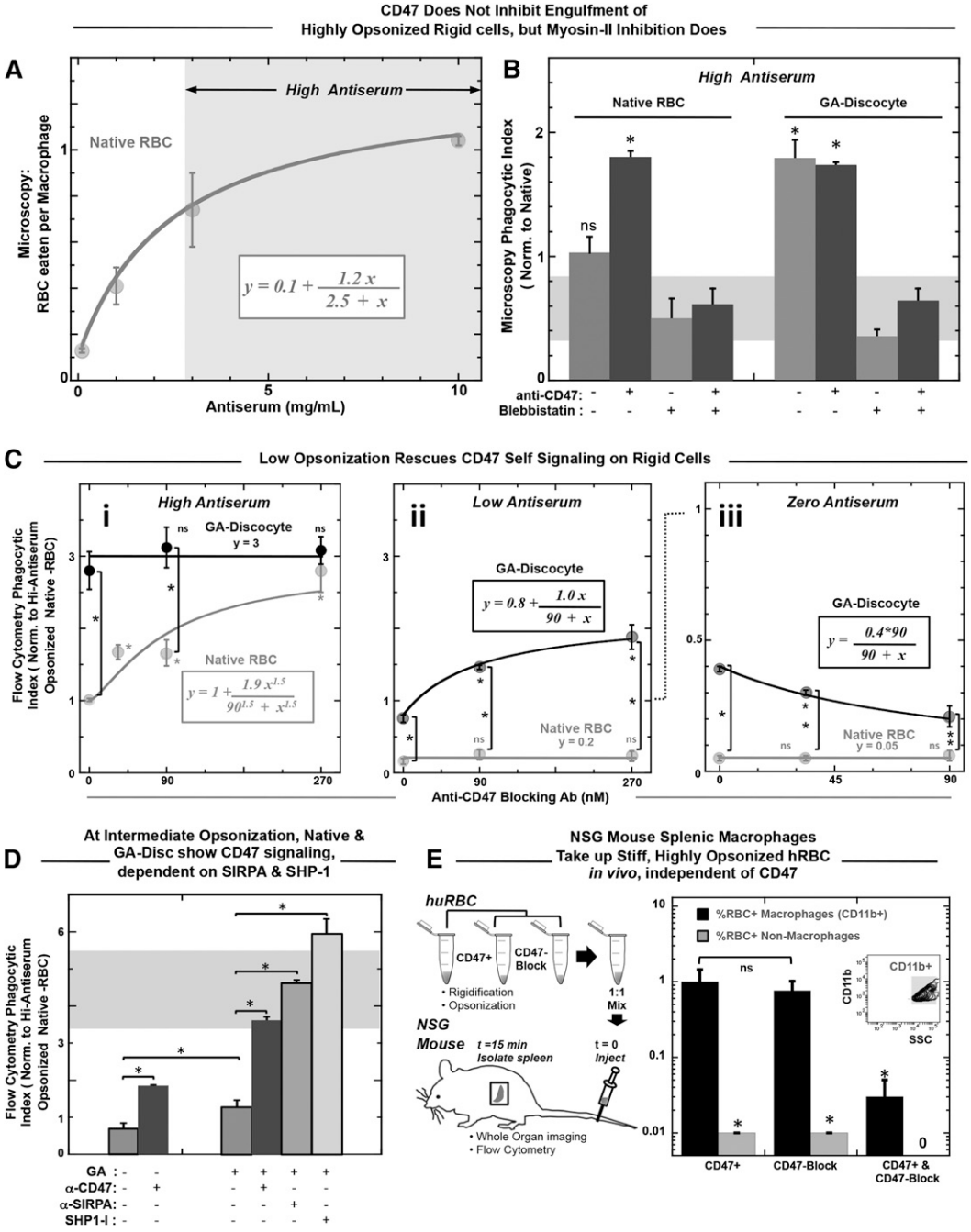

Figure 4. Rigid RBCs and CD47-blocked RBCs both promote opsonization-driven phagocytosis unless myosin-II is directly inhibited. (A) Phagocytic uptake shows an increasing and saturating response to antiserum concentration. High antiserum is defined as treatment with antiserum concentration greater than that required to result in half of saturating levels of engulfment, as highlighted by the arrows and gray box. (B) High antiserum opsonized RBCs were incubated with THP-1 macrophages for 45 minutes at 37°C. A microscopy-based phagocytosis assay indicated that native RBCs were engulfed more so when they were CD47 blocked, unless macrophages were pretreated with blebbistatin (20 μM). Rigidified GA discocyte engulfment proved independent of CD47 blocking (*$P < .05$). However, engulfment of GA discocytes, like native RBCs, was inhibited by pretreating macrophages with blebbistatin. The gray bar thus highlights a baseline level of myosin-II-independent phagocytosis. Phagocytosis is significantly higher than baseline when RBC targets are either CD47 blocked or GA rigidified. Blebbistatin pretreatment of both native-blocked and rigid cells keep uptake at the baseline. (C) High-throughput flow cytometry assay for phagocytic uptake with opsonization per supplemental Table 2 shows that for high antiserum opsonization, phagocytosis of GA discocytes is unaffected by blocking of CD47 (not significant) (i), whereas at low antiserum opsonization, blocking of CD47 on GA discocytes does increase phagocytosis) (ii). For high antiserum opsonized deformable native RBCs, phagocytosis increases with blocking of CD47 (i), whereas, at low antiserum opsonization, phagocytosis of native cells is insignificant regardless of blocking CD47 (not significant) (ii). Hyperbolic fits for i and ii give $K = 90$ nM and an ~2.5-fold increase from baseline to saturation. Clearly, the anti-CD47 blocking treatment alone is not sufficient to drive engulfment of native RBCs. In the absence of antiserum, or with zero antiserum treatment, blocking CD47 on GA discocytes reduces phagocytosis (iii). This suggests the functional CD47-SIRPA interaction on rigidified cells indicated by the SIRPA binding studies here (Figure 1B). For all experiments, *$P < .05$; n ≥ 3 ± standard error of the mean). (D) At intermediate antiserum opsonization (supplemental Table 2), CD47 signaling can be blocked. Phagocytosis of native RBCs and rigid GA discocytes significantly increases on blocking with anti-CD47 (90 nM). An anti-SIRPA antibody (90 nM) and an SHP-1 inhibitor (NSC87877, 60 nM) enhance uptake of GA discocytes. (E) NSG splenic macrophages take up stiff, highly opsonized hRBCs in vivo, independent of CD47. High antiserum opsonized GA rigidified (17 mM) RBCs were anti-CD47 (CD47 block) treated or not ($CD47^+$), mixed 1:1, and injected into NSG mice via the tail vein (n = 4). Rigid discs were prelabeled with 2 lipophilic dyes, either DiR or PKH26, to be distinguished after mixing. Spleens were isolated 15 minutes after injection, dissociated, and analyzed by flow cytometry. Splenic macrophages were distinguished from splenocytes by Cd11b expression and quantified for the percentage positive RBC uptake. Although 1% of splenic macrophages were positive for CD47 blocked and $CD47^+$ hRBCs, double-positive macrophages were rare, as were positive nonmacrophage cells ($CD11b^-$).

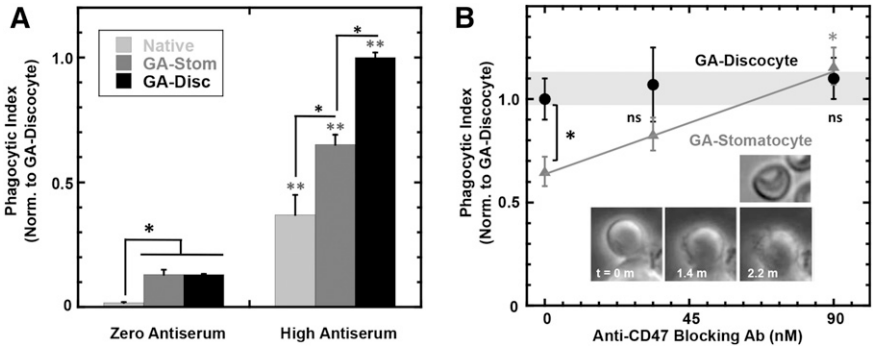

Figure 5. Shape of rigid RBCs modulates CD47's "don't eat me" signal. (A) A flow cytometry-based phagocytosis assay shows that macrophage phagocytosis of high antiserum opsonized native RBCs, GA stomatocytes, and GA discocytes is significantly higher than unopsonized cells (*$P < .05$ compares indicated conditions; ** $P < .05$ compares high antiserum to zero antiserum for each RBC condition: native RBC, GA stomatocytes, and GA discocytes). (B) RBCs treated with a mild hypotonic buffer followed by GA reaction generated rigid, more rounded, GA stomatocytes (upper inset image). A flow cytometry-based phagocytosis assay of high antiserum opsonized GA stomatocytes shows less engulfment than GA discocytes in the absence of anti-CD47 blocking antibody, whereas blocking CD47 equalized uptake (*$P < .05$; n ≥ 5000 macrophage in duplicate, ±SD). Time-lapse imaging of the macrophage phagocytic synapse with the stomatocyte shows pseudopods closely surrounding the rounded cell (lower inset image).

with GA stomatocytes (Figure 5B) is less effective than that seen with native cells (Figure 4Ci).

With anti-CD47 and high antiserum opsonization, both GA discocytes and GA stomatocytes are engulfed to a similar extent (Figure 5A). In contrast, GA discocytes are engulfed less than GA stomatocytes when opsonized with IgG from purified antiserum (supplemental Figure 5D), even though the amount of bound IgG on antiserum and pure IgG opsonization is the same (supplemental Figure 5D, inset). The latter result is consistent with IgG-opsonized spheres being phagocytosed more readily than nonspheres in studies of particles.[66] The difference may be explained by the fact that antiserum contains additional opsonizing factors, such as C3b,[65] that drive complement-receptor mediated phagocytosis characterized by large phagosomes in which the macrophage loosely surrounds the target[67,68] and minimizes the dense focal adhesions of IgG-driven phagocytosis.[69] The biconcave contour of a rigid GA discocyte and the resulting nonuniform membrane contact with a macrophage (supplemental Figure 3D) make complement-driven uptake more efficient. The loose contact between macrophage and a GA discocyte (supplemental Figure 3D) clearly contrasts with the tightly apposed pseudopods seen during GA stomatocyte engulfment (Figure 5B, inset).

Discussion

In many disease states and numerous conditions (eg, alcohol consumption), erythrocytes have been amply demonstrated to exhibit increased rigidity, opsonization, and clearance (supplemental Table 1), and numerous additional diseases (eg, Fanconi anemia[70]) have also been speculated to increase RBC rigidity. The quantitative balance between physicochemical changes of RBCs that promote phagocytosis vs CD47-SIRPA that signals against phagocytosis is summarized in a structure-function heat map that facilitates objective comparisons of the different phenotypes (columns in Figure 6A). The few differences in uptake evident for native RBCs vs rigid GA discocytes when myosin-II is inhibited reveal uptake of GA RBCs without red cell deformation and also a tendency of GA discocytes to stimulate stress fiber assembly even though myosin-IIA's ATPase is inhibited. At the opposite end of the heat map, blocking of CD47 has little effect on the uptake of GA discocytes (compare $CD47^-$ to $CD47^+$), with a slight attenuation of the uptake phenotype for blocked cells, perhaps reflecting the fact that blocking impedes the weakly adhesive interactions of CD47 with macrophage SIRPA.[7] Native CD47-blocked RBCs show an intermediate heat map profile but group more with the rigid GA discocytes, consistent with strong myosin-II activation.

For all of the various RBC targets, IgG on the RBCs is likely recognized by the macrophage receptor FcγRIIA, which triggers phagocytic cup formation independent of myosin-II (Figure 6B). The flexible native RBCs show that CD47-SIRPA inhibition dominates the opsonization signaling that otherwise activates myosin-II. Blocking CD47 on soft RBCs leads to the characteristic hourglass deformations seen when native RBCs from different species are engulfed,[71] consistent with CD47-SIRPA interactions being species specific.[7,72,73] Macrophages cannot deform GA-rigidified discocytes, which induces myosin-II activation, assembly, and accumulation at the phagocytic synapse, contributing to rapid rotation of the target in en face ingestion. Loss of RBC deformability contributes to rapid clearance of RBCs from the circulation,[36,41] consistent with rapid removal of rigid apoptotic bodies,[67,68] but the relative contributions of cell stiffness, opsonin density, and even the roles of macrophages are rarely clear. Rapid uptake can limit signaling from other receptor-ligand interactions as can a rigid discocyte's concave shape, which limits contact between the macrophage's nascent phagosome membrane and a target membrane as shown here (supplemental Figure 3D). A more spherical RBC shape indeed rescues CD47-SIRPA-mediated signaling (Figure 5B), consistent with the more tightly apposed projections seen with rounded GA stomatocytes (Figure 5B, bottom inset). Rigid polystyrene spheres with CD47 attached in the same way signal self, minimizing macrophage uptake in vitro and in vivo while also suppressing myosin-IIA localization to the phagocytic synapse.[7,12] FcγR-mediated adhesion seems analogous to the rapid kinase-driven adhesion mediated by integrins that can be amplified into focal adhesions when rigid substrates are engaged by myosin-II contractility[44,47]; however, the slower phosphatase signaling of CD47-SIRPA subsequently benefits from the high contact area and eventually dominates prophagocytic processes—unless some threshold for phagocytosis is already crossed in such a kinetic competition mechanism.

The various molecular and cellular processes described here all suggest a myosin-IIA regulatory pathway from unassembled and relaxed states of assembly to contracting fibers that make phagocytosis efficient (Figure 6C). Blebbistatin appears to block only the last step (contraction), as imaging after blebbistatin treatment still shows fibers, albeit relaxed fibers (Figure 3C). The CD47 pathway and target rigidity oppositely regulate at least the earlier steps (Figure 6C).

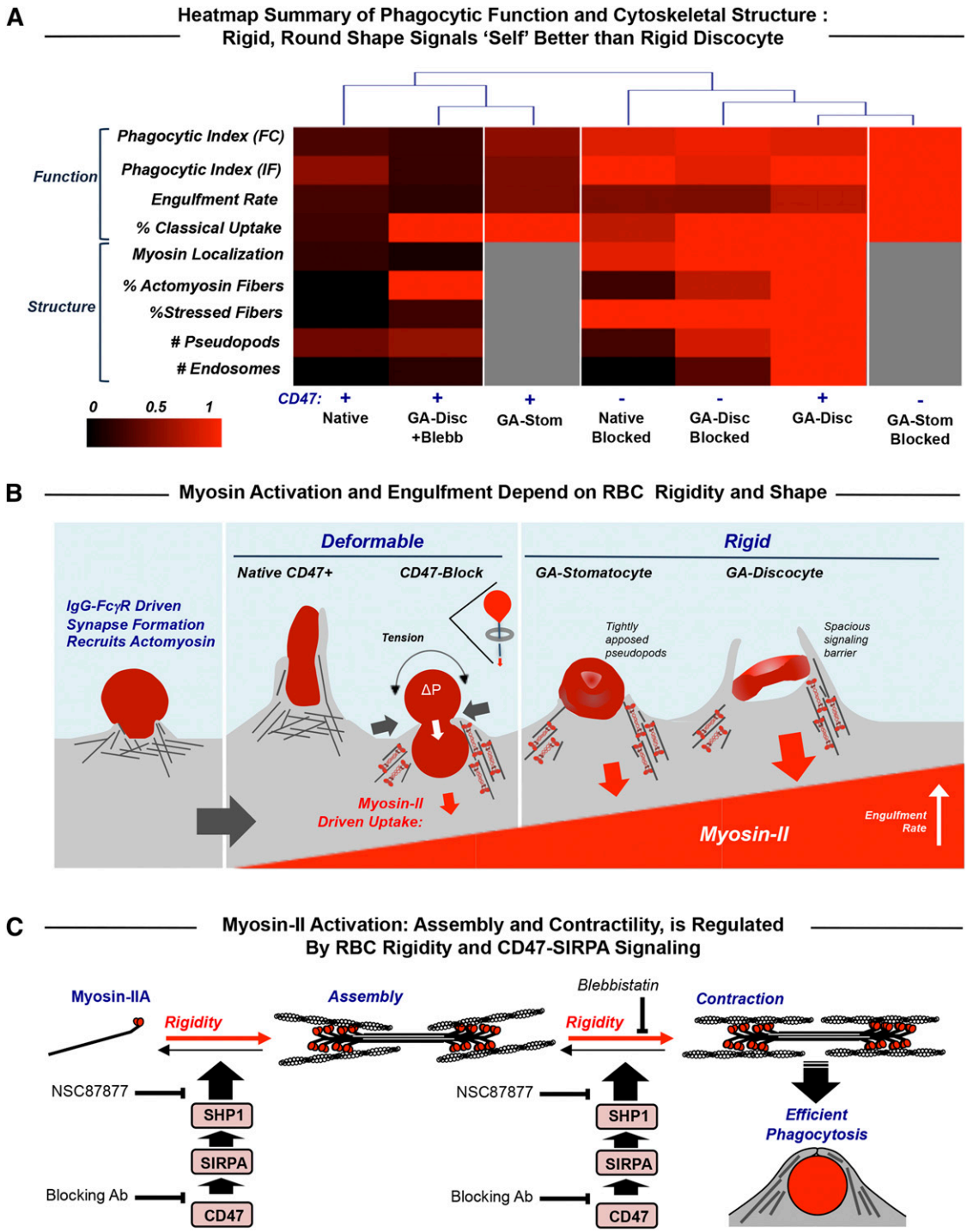

Figure 6. Myosin-II activity at the phagocytic synapse with opsonized RBC targets is inhibited by CD47 and enhanced by target rigidity. (A) Heat map summary and hierarchical clustering of normalized results for the various experiments. The dendrogram indicates that the macrophage response to rigid GA discocytes is distinct from that of native RBC targets and that blocking CD47 on deformable RBCs (but not on GA discocytes) reduces the difference, as does blebbistatin pretreatment of macrophages encountering GA discocytes (CD47$^+$ GA-Disc +Blebb). CD47 inhibition is partially rescued with rigid but rounded GA stomatocytes (CD47$^+$ GA-Stom), unless CD47 blocked (CD47$^-$ GA-Stom). (B) Macrophage recognition of IgG opsonin on the surface of RBCs by FcγR phagocytic receptors activates cytoskeletal proteins including myosin-II. Effective signaling via SIRPA to phosphatases does occur with CD47 on either flexible self-cells or sufficiently rounded but rigid self-cells. RBC rigidity has the effect of rapidly and strongly activating adhesion and myosin-II contractions. Macrophages pinch deformable CD47-blocked native RBCs at their midpoint and then fully engulf these RBCs in a manner analogous to a deflated balloon pulled through a napkin ring (inset schematic). Rigid discocytes maintain their shape throughout engulfment, which limits contact between macrophage receptors and ligands, particularly SIRPA and CD47 on the RBCs, and thus the spacious phagosome may act as a signaling barrier. Rounded GA stomatocytes show tightly apposed macrophage pseudopods and rescued CD47 signaling. (C) Schematic of myosin-II assembly in phagocytosis in which myosin-II dimers assemble and contract actin filaments in response to rigidity of human RBCs while becoming more disorganized in response to CD47-SIRPA-mediated activation of immunoinhibitory phosphatase, SHP-1. We showed previously[7] that phosphorylation of tyrosines in myosin-IIA's head and tail activate the motor, increasing its accumulation at the phagocytic synapse and increasing the efficiency of phagocytic uptake, whereas CD47-SIRPA's activation of the tyrosine phosphatase SHP-1 deactivates myosin-IIA. Blebbistatin blocks the activity of myosin II ATPase and thus the ability of the head to generate contractile forces, relaxing the assembled actomyosin fibers. The SHP-1 inhibitor NSC87877 reduces inhibition by CD47 and thus increases RBC uptake.

Loss of deformability of aged erythrocytes has long been thought to contribute to their clearance from circulation, with additional determinants possibly including partial loss of CD47 (6-50%[74-76]) and perhaps oxidation of CD47.[77,78] Gain of deformability might also be crucial to erythropoiesis,[30] particularly release from marrow macrophages,[31] which is certainly relevant to many efforts aimed at making circulating RBCs from stem cell cultures.[29] The results here clarify the complementary role that target deformability plays in clearance by tissue macrophages. The findings are likely relevant to chemotherapy-rigidified leukemias, rigid-walled microbes (yeast and bacteria), various viral and nonviral particles used in gene and drug delivery, and the well-known rigid RBCs that result from blood storage and that also occur in common diseases such as sickle cell and thalassemia.

Acknowledgments

This work was supported by the National Institutes of Health, National Institute of Biomedical Imaging and Bioengineering (grant R01-EB007049), National Heart, Lung, and Blood Institute (grant R01-HL124106), National Institute of Diabetes and Digestive and Kidney Diseases (grants P01-DK032094 and P30-DK090969), National Center for Advancing Translational Sciences (grant 8UL1TR000003); the National Science Foundation (Materials Research Science and Engineering Center and Nano Science and Engineering Center-Nano Bio Interface Center), and an International Research Training Group grant 1524.

Authorship

Contribution: N.G.S. and A.M.B. performed experiments; N.G.S. and T.R. analyzed results; N.G.S. and D.E.D. created figures and wrote the paper; and N.G.S., R.D., R.L., and D.E.D. designed the research.

Conflict-of-interest disclosure: The authors declare no competing financial interests.

Correspondence: Dennis E. Discher, University of Pennsylvania, 220 S 33rd St, 129 Towne Building, Philadelphia, PA 19104; e-mail: discher@seas.upenn.edu.

References

1. Ravetch JV, Lanier LL. Immune inhibitory receptors. *Science.* 2000;290(5489):84-89.
2. Vicente-Manzanares M, Sánchez-Madrid F. Role of the cytoskeleton during leukocyte responses. *Nat Rev Immunol.* 2004;4(2):110-122.
3. Swanson JA. Shaping cups into phagosomes and macropinosomes. *Nat Rev Mol Cell Biol.* 2008; 9(8):639-649.
4. Flannagan RS, Jaumouillé V, Grinstein S. The cell biology of phagocytosis. *Annu Rev Pathol.* 2012; 7:61-98.
5. Olazabal IM, Caron E, May RC, Schilling K, Knecht DA, Machesky LM. Rho-kinase and myosin-II control phagocytic cup formation during CR, but not FcgammaR, phagocytosis. *Curr Biol.* 2002;12(16):1413-1418.
6. Araki N, Hatae T, Furukawa A, Swanson JA. Phosphoinositide-3-kinase-independent contractile activities associated with Fcgamma-receptor-mediated phagocytosis and macropinocytosis in macrophages. *J Cell Sci.* 2003;116(Pt 2):247-257.
7. Tsai RK, Discher DE. Inhibition of "self" engulfment through deactivation of myosin-II at the phagocytic synapse between human cells. *J Cell Biol.* 2008;180(5):989-1003.
8. Jiang P, Lagenaur CF, Narayanan V. Integrin-associated protein is a ligand for the P84 neural adhesion molecule. *J Biol Chem.* 1999;274(2): 559-562.
9. Veillette A, Thibaudeau E, Latour S. High expression of inhibitory receptor SHPS-1 and its association with protein-tyrosine phosphatase SHP-1 in macrophages. *J Biol Chem.* 1998; 273(35):22719-22728.
10. Okazawa H, Motegi S, Ohyama N, et al. Negative regulation of phagocytosis in macrophages by the CD47-SHPS-1 system. *J Immunol.* 2005;174(4): 2004-2011.
11. Baba T, Fusaki N, Shinya N, Iwamatsu A, Hozumi N. Myosin is an in vivo substrate of the protein tyrosine phosphatase (SHP-1) after mIgM cross-linking. *Biochem Biophys Res Commun.* 2003; 304(1):67-72.
12. Rodriguez PL, Harada T, Christian DA, Pantano DA, Tsai RK, Discher DE. Minimal "Self" peptides that inhibit phagocytic clearance and enhance delivery of nanoparticles. *Science.* 2013; 339(6122):971-975.
13. Oldenborg PA, Gresham HD, Lindberg FP. CD47-signal regulatory protein α (SIRPalpha) regulates Fcgamma and complement receptor-mediated phagocytosis. *J Exp Med.* 2001;193(7):855-862.
14. Gardai SJ, McPhillips KA, Frasch SC, et al. Cell-surface calreticulin initiates clearance of viable or apoptotic cells through trans-activation of LRP on the phagocyte. *Cell.* 2005;123(2):321-334.
15. Blazar BR, Lindberg FP, Ingulli E, et al. CD47 (integrin-associated protein) engagement of dendritic cell and macrophage counterreceptors is required to prevent the clearance of donor lymphohematopoietic cells. *J Exp Med.* 2001; 194(4):541-549.
16. Jaiswal S, Jamieson CH, Pang WW, et al. CD47 is upregulated on circulating hematopoietic stem cells and leukemia cells to avoid phagocytosis. *Cell.* 2009;138(2):271-285.
17. Weiskopf K, Ring AM, Ho CC, et al. Engineered SIRPα variants as immunotherapeutic adjuvants to anticancer antibodies. *Science.* 2013; 341(6141):88-91.
18. Kay MM. Mechanism of removal of senescent cells by human macrophages in situ. *Proc Natl Acad Sci USA.* 1975;72(9):3521-3525.
19. Turrini F, Arese P, Yuan J, Low PS. Clustering of integral membrane proteins of the human erythrocyte membrane stimulates autologous IgG binding, complement deposition, and phagocytosis. *J Biol Chem.* 1991;266(35): 23611-23617.
20. Oldenborg PA, Zheleznyak A, Fang YF, Lagenaur CF, Gresham HD, Lindberg FP. Role of CD47 as a marker of self on red blood cells. *Science.* 2000; 288(5473):2051-2054.
21. Lutz HU. Innate immune and non-immune mediators of erythrocyte clearance. *Cell Mol Biol (Noisy-le-grand).* 2004;50(2):107-116.
22. Bosman GJ, Werre JM, Willekens FL, Novotný VM. Erythrocyte ageing in vivo and in vitro: structural aspects and implications for transfusion. *Transfus Med.* 2008;18(6):335-347.
23. Hod EA, Zhang N, Sokol SA, et al. Transfusion of red blood cells after prolonged storage produces harmful effects that are mediated by iron and inflammation. *Blood.* 2010;115(21):4284-4292.
24. Mohandas N, Gallagher PG. Red cell membrane: past, present, and future. *Blood.* 2008;112(10): 3939-3948.
25. Reliene R, Mariani M, Zanella A, et al. Splenectomy prolongs in vivo survival of erythrocytes differently in spectrin/ankyrin- and band 3-deficient hereditary spherocytosis. *Blood.* 2002;100(6):2208-2215.
26. Chasis JA, Mohandas N. Erythrocyte membrane deformability and stability: two distinct membrane properties that are independently regulated by skeletal protein associations. *J Cell Biol.* 1986; 103(2):343-350.
27. Mohandas N, Evans E. Mechanical properties of the red cell membrane in relation to molecular structure and genetic defects. *Annu Rev Biophys Biomol Struct.* 1994;23:787-818.
28. Raat NJ, Ince C. Oxygenating the microcirculation: the perspective from blood transfusion and blood storage. *Vox Sang.* 2007;93(1):12-18.
29. Giarratana MC, Marie T, Darghouth D, Douay L. Biological validation of bio-engineered red blood cell productions. *Blood Cells Mol Dis.* 2013;50(2): 69-79.
30. Leblond PF, Lacelle PL, Weed RI. Cellular deformability: a possible determinant of the normal release of maturing erythrocytes from the bone marrow. *Blood.* 1971;37(1):40-46.
31. Chasis JA, Mohandas N. Erythroblastic islands: niches for erythropoiesis. *Blood.* 2008;112(3): 470-478.
32. Bercoff J, Chaffai S, Tanter M, et al. In vivo breast tumor detection using transient elastography. *Ultrasound Med Biol.* 2003;29(10):1387-1396.
33. Lam WA, Rosenbluth MJ, Fletcher DA. Chemotherapy exposure increases leukemia cell stiffness. *Blood.* 2007;109(8):3505-3508.
34. Cross SE, Jin YS, Rao J, Gimzewski JK. Nanomechanical analysis of cells from cancer patients. *Nat Nanotechnol.* 2007;2(12):780-783.
35. Beningo KA, Wang YL. Fc-receptor-mediated phagocytosis is regulated by mechanical properties of the target. *J Cell Sci.* 2002;115(Pt 4): 849-856.
36. Jain SK, Mohandas N, Clark MR, Shohet SB. The effect of malonyldialdehyde, a product of lipid peroxidation, on the deformability, dehydration

and 51Cr-survival of erythrocytes. *Br J Haematol.* 1983;53(2):247-255.

37. Hebbel RP, Miller WJ. Phagocytosis of sickle erythrocytes: immunologic and oxidative determinants of hemolytic anemia. *Blood.* 1984; 64(3):733-741.
38. Salem M, Mauguen Y, Prangé T. Revisiting glutaraldehyde cross-linking: the case of the Arg-Lys intermolecular doublet. *Acta Crystallogr Sect F Struct Biol Cryst Commun.* 2010;66(Pt 3): 225-228.
39. Ballas SK, Mohandas N. Pathophysiology of vaso-occlusion. *Hematol Oncol Clin North Am.* 1996;10(6):1221-1239.
40. Tsai M, Kita A, Leach J, et al. In vitro modeling of the microvascular occlusion and thrombosis that occur in hematologic diseases using microfluidic technology. *J Clin Invest.* 2012;122(1):408-418.
41. Deplaine G, Safeukui I, Jeddi F, et al. The sensing of poorly deformable red blood cells by the human spleen can be mimicked in vitro. *Blood.* 2011; 117(8):88-95.
42. Mebius RE, Kraal G. Structure and function of the spleen. *Nat Rev Immunol.* 2005;5(8):606-616.
43. Merkel TJ, Jones SW, Herlihy KP, et al. Using mechanobiological mimicry of red blood cells to extend circulation times of hydrogel microparticles. *Proc Natl Acad Sci USA.* 2011; 108(2):586-591.
44. Shin JW, Buxboim A, Spinler KR, et al. Contractile forces sustain and polarize hematopoiesis from stem and progenitor cells. *Cell Stem Cell.* 2014; 14(1):81-93.
45. Féréol S, Fodil R, Labat B, et al. Sensitivity of alveolar macrophages to substrate mechanical and adhesive properties. *Cell Motil Cytoskeleton.* 2006;63(6):321-340.
46. Oakes PW, Patel DC, Morin NA, et al. Neutrophil morphology and migration are affected by substrate elasticity. *Blood.* 2009;114(7): 1387-1395.
47. Engler AJ, Sen S, Sweeney HL, Discher DE. Matrix elasticity directs stem cell lineage specification. *Cell.* 2006;126(4):677-689.
48. Hod EA, Brittenham GM, Billote GB, et al. Transfusion of human volunteers with older, stored red blood cells produces extravascular hemolysis and circulating non-transferrin-bound iron. *Blood.* 2011;118(25):6675-6682.
49. Rutala WA, Weber DJ, Healthcare Infection Control Practices Advisory Committee. Guideline for disinfection and sterilization in healthcare facilities. Available at: http://www.cdc.gov/hicpac/pdf/guidelines/disinfection_nov_2008.pdf. Accessed November 28, 2014.
50. Di Stefano F, Siriruttanapruk S, McCoach J, Burge PS. Glutaraldehyde: an occupational hazard in the hospital setting. *Allergy.* 1999; 54(10):1105-1109.
51. Li J, Dao M, Lim CT, Suresh S. Spectrin-level modeling of the cytoskeleton and optical tweezers stretching of the erythrocyte. *Biophys J.* 2005; 88(5):3707-3719.
52. Lo CM, Buxton DB, Chua GC, Dembo M, Adelstein RS, Wang YL. Nonmuscle myosin IIb is involved in the guidance of fibroblast migration. *Mol Biol Cell.* 2004;15(3):982-989.
53. Raab M, Swift J, Dingal PC, Shah P, Shin JW, Discher DE. Crawling from soft to stiff matrix polarizes the cytoskeleton and phosphoregulates myosin-II heavy chain. *J Cell Biol.* 2012;199(4): 669-683.
54. Patel NR, Bole M, Chen C, et al. Cell elasticity determines macrophage function. *PLoS ONE.* 2012;7(9):e41024.
55. Blakney AK, Swartzlander MD, Bryant SJ. The effects of substrate stiffness on the in vitro activation of macrophages and in vivo host response to poly(ethylene glycol)-based hydrogels. *J Biomed Mater Res A.* 2012;100(6): 1375-1386.
56. Lammel U, Bechtold M, Risse B, et al. The Drosophila FHOD1-like formin Knittrig acts through Rok to promote stress fiber formation and directed macrophage migration during the cellular immune response. *Development.* 2014;141(6): 1366-1380.
57. Tanner K, Boudreau A, Bissell MJ, Kumar S. Dissecting regional variations in stress fiber mechanics in living cells with laser nanosurgery. *Biophys J.* 2010;99(9):2775-2783.
58. Sen S, Tewari M, Zajac A, Barton E, Sweeney HL, Discher DE. Upregulation of paxillin and focal adhesion signaling follows Dystroglycan Complex deletions and promotes a hypertensive state of differentiation. *Eur J Cell Biol.* 2011;90(2-3): 249-260.
59. Christian JA, Rebar AH, Boon GD, Low PS. Senescence of canine biotinylated erythrocytes: increased autologous immunoglobulin binding occurs on erythrocytes aged in vivo for 104 to 110 days. *Blood.* 1993;82(11):3469-3473.
60. Rettig MP, Low PS, Gimm JA, Mohandas N, Wang J, Christian JA. Evaluation of biochemical changes during in vivo erythrocyte senescence in the dog. *Blood.* 1999;93(1):376-384.
61. Franco RS, Puchulu-Campanella ME, Barber LA, et al. Changes in the properties of normal human red blood cells during in vivo aging. *Am J Hematol.* 2013;88(1):44-51.
62. Tada K, Tanaka M, Hanayama R, et al. Tethering of apoptotic cells to phagocytes through binding of CD47 to Src homology 2 domain-bearing protein tyrosine phosphatase substrate-1. *J Immunol.* 2003;171(11):5718-5726.
63. Da Costa L, Galimand J, Fenneteau O, Mohandas N. Hereditary spherocytosis, elliptocytosis, and other red cell membrane disorders. *Blood Rev.* 2013;27(4):167-178.
64. Smith BD, Segel GB. Abnormal erythrocyte endothelial adherence in hereditary stomatocytosis. *Blood.* 1997;89(9):3451-3456.
65. Janeway CA Jr, Travers P, Walport M, et al. Immunobiology: The Immune System in Health and Disease. New York: Garland Science; 2001.
66. Champion JA, Mitragotri S. Role of target geometry in phagocytosis. *Proc Natl Acad Sci USA.* 2006;103(13):4930-4934.
67. deCathelineau AM, Henson PM. The final step in programmed cell death: phagocytes carry apoptotic cells to the grave. *Essays Biochem.* 2003;39:105-117.
68. Erwig LP, Henson PM. Clearance of apoptotic cells by phagocytes. *Cell Death Differ.* 2008; 15(2):243-250.
69. Allen LA, Aderem A. Molecular definition of distinct cytoskeletal structures involved in complement- and Fc receptor-mediated phagocytosis in macrophages. *J Exp Med.* 1996;184(2):627-637.
70. Malorni W, Straface E, Pagano G, et al. Cytoskeleton alterations of erythrocytes from patients with Fanconi's anemia. *FEBS Lett.* 2000; 468(2-3):125-128.
71. Swanson JA, Johnson MT, Beningo K, Post P, Mooseker M, Araki N. A contractile activity that closes phagosomes in macrophages. *J Cell Sci.* 1999;112(Pt 3):307-316.
72. Subramanian S, Parthasarathy R, Sen S, Boder ET, Discher DE. Species- and cell type-specific interactions between CD47 and human SIRPalpha. *Blood.* 2006;107(6):2548-2556.
73. Takenaka K, Prasolava TK, Wang JCY, et al. Polymorphism in Sirpa modulates engraftment of human hematopoietic stem cells. *Nat Immunol.* 2007;8(12):1313-1323.
74. Anniss AM, Sparrow RL. Expression of CD47 (integrin-associated protein) decreases on red blood cells during storage. *Transfus Apheresis Sci.* 2002;27(3):233-238.
75. Kamel N, Goubran F, Ramsis N, Ahmed AS. Effects of storage time and leucocyte burden of packed and buffy-coat depleted red blood cell units on red cell storage lesion. *Blood Transfus.* 2010;8(4):260-266.
76. Stewart A, Urbaniak S, Turner M, Bessos H. The application of a new quantitative assay for the monitoring of integrin-associated protein CD47 on red blood cells during storage and comparison with the expression of CD47 and phosphatidylserine with flow cytometry. *Transfusion.* 2005;45(9):1496-1503.
77. Olsson M, Oldenborg PA. CD47 on experimentally senescent murine RBCs inhibits phagocytosis following Fcgamma receptor-mediated but not scavenger receptor-mediated recognition by macrophages. *Blood.* 2008; 112(10):4259-4267.
78. Burger P, Hilarius-Stokman P, de Korte D, van den Berg TK, van Bruggen R. CD47 functions as a molecular switch for erythrocyte phagocytosis. *Blood.* 2012;119(23):5512-5521.

2015 125: 542-552
doi:10.1182/blood-2014-06-585299 originally published online November 19, 2014

Cell rigidity and shape override CD47's "self"-signaling in phagocytosis by hyperactivating myosin-II

Nisha G. Sosale, Tahereh Rouhiparkouhi, Andrew M. Bradshaw, Rumiana Dimova, Reinhard Lipowsky and Dennis E. Discher

Blood (print ISSN 0006-4971, online ISSN 1528-0020), is published weekly by the American Society of Hematology, 2021 L St, NW, Suite 900, Washington DC 20036.